Periodico di Mineralogia Volume 93, No. 6, 2024
ISSN: 0369-8963

Phase equilibria, thermal and microstructural studies on organic analog of a nonmetal-nonmetal monotectic alloy; 2-cyanoacetamide-4-bromonitrobenzene system

Birusanti Arun Babu[*1] *Nabisabgari Hussain Basha*[2] *and Mala Sreenivasulu*[1]

[1]*Department of Chemistry, Rajeev Gandhi Memorial College of Engineering and Technology (Autonomous), Nandyal-518501, Andhra Pradesh, India*

[2]*Department of Humanities and Sciences, CVR College of Engineering, Hyderabad, 501510 India*

ABSTRACT

The phase diagram of 2-cyanoacetamide―4-bromonitrobezene system was studied which shows a large miscibility gap and the formation of a eutectic and a monotectic where the mole fractions of 2-cyanoacetamide are 0.92 and 0.065, respectively. The critical temperature is being 63.5^{o}C above the monotectic horizontal line. Growth kinetics of the pure components and the binary mixtures (monotectic and eutectic) studied by measuring the rate of movement (v) of solid-liquid interface in a thin U-tube at different undercoolings (ΔT) suggests the applicability of the Hillig-Turnbull's equation. The thermal properties of materials such as heat of mixing, entropy of fusion, roughness parameter, interfacial energy and excess thermodynamic functions were computed from the enthalpy of fusion values, determined by differential scanning calorimeter (Mettler DSC-4000) system. The solid-liquid interfacial energy data confirm the applicability of the Cahn non-wetting condition. The microstructures of monotectic and eutectics were taken and have also been explained.

Key words: Phase diagram; Monotectic alloys; Eutectic; Thermal properties; Interfacial energy; Microstructure.

 https://doi.org/10.5281/zenodo.14191038

1. Introduction

The investigations on the temperature dependent solidification behaviour of monotectic alloy are of potential importance for fundamental investigations for self lubricating alloys and various industrial applications [1-3]. Due to high transformation temperature and wide density difference, the metallic systems do not constitute an interesting area of investigations [4-5]. However, due low transformation temperature, ease of purification, transparency, wider choice of materials and minimized convection effects on solidification, organic systems are being used as model systems for detailed investigation of the parameters which control the mechanism of solidification which decides the properties of materials. But now-a-days organic systems are known for promising NLO, fluorescence, and conducting behavior which reinforce the investigation to produce the different materials for their specific device applications [6-9]. With this view, the number of research group [10-12] is working on organic systems to explore the different properties for specific applications.

Due to several difficulties associated with systems forming monotectics, these alloys have been studies to a very small extent. Nonetheless, some of the articles [1, 13-14] explain various interesting phenomenon of monotectic alloys. As pointed out, the wide freezing range and large density difference between two liquid phases are the main problems. In addition, the role of wetting behaviour, interfacial energy, thermal conductivity and buoyancy during the phase separation process has been a subject of great discussion. 4-bromonitrobenzene (BCB) and 2-cyanoacetamide (CA) are the organic materials having high enthalpy of fusion (21.59 and 18.97 kJ. mol^{-1} respectively) values as compared to metallic compounds where the heat of fusion value, is less than 4.0 kJ. mol^{-1}, and therefore the present system might be considered as organic analog of nonmetal-nonmetal systems. In the present communication, the details of phase

 https://doi.org/10.5281/zenodo.14191038

diagram, growth kinetic study at different undercoolings, heat of fusion, Jackson's roughness parameter, interfacial energy, excess thermodynamic functions and microstructures are reported.

2. Experimental

2.1. Materials and purification

2-Cyanoacetamide (Aldrich, Germany), was purified by crystallization from de-ionized water while 4-bromonitrobenzene (Aldrich, Germany) was purified by crystallization from ethanol. The melting temperatures of CA and BNB were found to be 121.0 and 128.5 ^{o}C, respectively, which are close to their reported values [15].

2.2. Phase diagram

The phase diagram of BNB-CA system was determined by recording the melting point temperature of mixtures in the entire range of composition of BNB-CA and plotting a curve in composition on the X-axis and their respective melting/complete miscibility temperature on the Y-axis. In this method [16-17] mixtures of two components covering the entire range of compositions were prepared and taken in test tubes and after sealing the mouth of the test tubes these mixtures were homogenized 4 times by repeating the process of melting followed by chilling in ice cooled water. The melting/complete miscible temperatures of different composition were determined using a melting point apparatus (Toshniwal) attached with a precision thermometer associated with an accuracy of ± 0.5 ^{o}C. The determined numerical data of solid-liquid and liquid-liquid equilibrium of different composition and temperatures are given in Table 1.

 https://doi.org/10.5281/zenodo.14191038

ISSN: 0369-8963

2.3. Enthalpy of fusion

The heat of fusion of the pure components, the eutectic and the monotectic were determined [18] by differential scanning calorimeter (Mettler DSC-4000 system). Indium and zinc samples were used to calibrate the DSC unit. The amount of test sample and heating rate were about 7 mg and 5 ^{o}C min^{-1}, respectively. The values of enthalpy of fusion are reproducible within ± 1.0 %.

2.4. Growth kinetics

The growth kinetics of BNB, CA and their eutectic and monotectic were studied [17-18] by measuring the rate of movement of the solid–liquid interface at different undercoolings in a U-shape capillary tube of Jena glass of 150 mm horizontal portion and 5 mm internal diameter. Molten samples of pure components, eutectic and monotectic were separately taken in the capillary, and placed in a silicone oil bath. The temperature of the oil bath was maintained using microprocessor temperature controller of accuracy ±0.1 ^{o}C. At a particular temperature, below the melting point of the sample, a seed crystal of the same composition was added at one end of the U-tube, to facilitate the nucleation and the rate of movement of the solid–liquid interface was measured using a traveling microscope and a stop watch.

2.5. Microstructure

Microstructures of the eutectic and the monotectic were recorded [26] by placing a drop of molten compound on a hot glass slide. To avoid the inclusion of the impurities from the atmosphere and formation of bubbles, a cover slip was glided over the melt and it was allowed to cool to get a super cooled liquid. The melt was nucleated with a seed crystal of the same

 https://doi.org/10.5281/zenodo.14191038

ISSN: 0369-8963

composition taking care for unidirectional freezing. The unidirectionally solidified sample on glass slide was then placed on the platform of an optical microscope (Leitz Labourlux D). The different regions of the glass slide were viewed and photographs of interesting region were recorded choosing suitable magnification using a camera attached with the microscope.

3. Results and discussions

3.1. Phase diagram

The melting points of pure compounds BNB and CA are represented in the extreme left and right sides of the diagram at 128.5 and 121 ^{o}C, respectively. The melting point of BNB decreases with addition of CA up to M (the monotectic point), after which, even a slight addition of CA cause the appearance of two immiscible layers (Fig.1). In this figure the immiscibility region is shown by the area $L_1 + L_2$ bounded by the curve MCM_h. The point C at the top of the curve is the critical point or consolute point and the corresponding temperature (188 ^{o}C) is known as critical solution temperature (T_c). The miscibility temperature starts increasing after M, attains its maximum point at C, and thereafter decreases till it attains the monotectic horizontal (M_h). The miscibility curve is still continued in the region ($S + L_2$) that lies between the eutectic and monotectic horizontal lines and end at the point E, the eutectic point. The area ($L_1 + L_2$) may be regarded as to be made up of an infinite number of tie lines which connect the two liquid phases L_1 and L_2 at the extreme sides of the diagram. These tie lines become progressively shorter until the ultimate tie line at the top of the area reduce to a point C that corresponds to the critical solution temperature. This system involves three types of phase separation processes: (i) $L \leftrightarrow L_1 + L_2$, (ii)$L_1 \rightleftharpoons S_1 + L_2$, (iii) $L_2 \rightleftharpoons S_1 + S_2$. First of these, concerns the phase separation

 https://doi.org/10.5281/zenodo.14191038

ISSN: 0369-8963

of liquid L in the two phase region (L_1 + L_2) as the liquid of the composition corresponding T_c is cooled below the critical solution temperature. The second reaction is the monotectic phase separation reaction and is similar to the eutectic reaction except that both the phases produced are not solids. This reaction occurs when a liquid of monotectic composition is cooled through the monotectic temperature, T_M. As a result of cooling below T_M the liquid L_1, which is rich in one component (BNB) decomposes into a solid phase S_1 rich in the first component and another liquid phase L_2 rich in the second component (CA). The third reaction is the eutectic reaction, when a liquid of eutectic composition is cooled below the eutectic temperature T_E, the phase separation reaction results in two solids S_1 and S_2.

The mole fraction of CA in eutectic and monotectic are 0.92 and 0.065 and their corresponding melting temperatures are 118.5 and 124.5^{o}C, respectively. The upper consolute/critical temperature (T_c) is 188.0 ^{o}C which is 63.5 ^{o}C above the monotectic horizontal (M_h). Above the critical temperature (T_c), the two components are miscible in all proportions. However, below T_c temperature and between 0.065 and 0.92 mole fraction of CA compositions range the two immiscible liquids (L_1 and L_2) are produced.

3.2. Growth kinetics

In order to study the crystallization behavior of the pure components and binary mixtures (the eutectic and the monotectic) was studies by measuring the linear velocity of crystallization (v) at different undercooling (ΔT) by observing the rate of movement of moving front in a capillary. The crystallization data are shown in Fig. 2 in the form of linear plots which are in accordance with the Hillig-Turnbull equation, [19],

$$v = u\,(\Delta T)^n \quad \ldots (1)$$

 https://doi.org/10.5281/zenodo.14191038

ISSN: 0369-8963

where u and n are constants depending on the solidification behaviour of the materials involved. The values of u and n in each case were determined from the intercepts and slope of the straight lines (Fig. 2). The determined experimental values of these constants are given in Table 2. The basic criterion for the growth mechanism [20] is the comparison of the temperature dependence of linear velocity of crystallization with the theoretically predicted, equations. While normal growth generally occurs on the rough interface in which case there is direct proportionality between the crystallization and under cooling, lateral growth is facilitated by the presence of steps, jogs, bends, etc. and under such condition the relationship for the spiral mechanism follows the parabolic law given by equation (1). While in the case of the eutectic and the monotectic, there is square relationship following parabolic law between linear growth velocity and undercooling, in the case of CA there is direct proportionality between the growth velocity and undercooling. In the case of BNB the growth velocity is very high in comparison to that of CA.

It is well know that a value of u gives measure of growth velocity of material. It is evident from the data reported in Table 1 that growth velocity of BNB is very high in comparison to that of CA and the value of the linear velocity of crystallization of the eutectic lie between two components while for monotectic it is higher than the two components. These findings may be explained by the mechanism given by Winegard et al. [21] where the crystallisation of eutectic/monotectic begins with the formation of the nucleus of one of the phases. This phase grows until the surrounding liquid becomes rich in the other component and a stage is reached when the second component start nucleating. Now there are two possibilities, either the two initial crystals grow side-by-side or there may be alternate nucleation of the two phases. The deviation of n values from 2, observed in some cases, is due to difference in temperature of bath

 https://doi.org/10.5281/zenodo.14191038

ISSN: 0369-8963

and temperature of growing interface. From the values of u (Table 2) it can be concluded that growth velocity of eutectic lies between those of the parent components. However, for monotectic it is higher than the parent components. These findings suggest that the two phases of monotectic and eutectic solidify by the side-by-side growth mechanism.

3.3. Thermochemistry

The knowledge of enthalpy of fusion values of the pure components, the eutectic and the monotectic are important in understanding the mechanism of solidification, structure of eutectic melt and the nature of interaction between two components forming the eutectic and the monotectic. In addition, different thermodynamic quantities such as entropy of fusion, interfacial energy, enthalpy of mixing, excess thermodynamic functions and Jackson's roughness parameter can be calculated from the entropy of fusion data. The values of enthalpy of fusion of the pure components, the eutectic and the monotectic, determined by the DSC method, are reported in Table 2. For comparison, the value of enthalpy of fusion of eutectic has been calculated by the mixture law [22]

$$\left(\Delta_f H\right)_{eut} = x_1.\Delta_f H_1^o + x_2.\Delta_f H_2^o \qquad \ldots. (2)$$

where x and $\Delta_f H$ are the mole fraction and heat of function, respectively of the component indicated by the subscript. The calculated enthalpy of fusion value is tabulated in Table 2. The value of enthalpy of mixing which is the difference of experimental and the calculated values of the enthalpy of fusion is found to be 0.95 KJmol^{-1}. As such, three types of structures are suggested [22]; quasi–eutectic for $\Delta_{mix}H > 0$, clustering of molecules for $\Delta_{mix}H < 0$ and molecular solution for $\Delta_{mix}H = 0$. In present system the positive value of $\Delta_{mix}H$ for the eutectic suggests the formation of quasi-eutectic structure in the binary melt of the eutectic [23]. The

 https://doi.org/10.5281/zenodo.14191038

ISSN: 0369-8963

entropy of fusion ($\Delta_{fus}S$) values, for different materials has been calculated by dividing the enthalpy of fusion by their corresponding absolute melting temperatures (Table 2).

A measure of deviation from ideal behaviour can be best expressed in terms of excess thermodynamic functions, namely, excess free energy (g^E), excess enthalpy (h^E), and excess entropy (s^E) which give a more quantitative idea about the nature of molecular interactions. The excess thermodynamic functions could be calculated [16, 24-25] using the following equations and the values are given in Table 3:

$$g^{E} = RT\left[x_1 \ln\gamma_1^{l} + x_2 \ln\gamma_2^{l}\right] \quad \text{... (3)}$$

$$h^{E} = -RT^2\left[x_1 \frac{\partial \ln\gamma_1^{l}}{\partial T} + x_2 \frac{\partial \ln\gamma_2^{l}}{\partial T}\right] \quad \text{... (4)}$$

$$s^{E} = -R\left[x_1 \ln\gamma_1^{l} + x_2 \ln\gamma_2^{l} + x_1 T \frac{\partial \ln\gamma_1^{l}}{\partial T} + x_2 T \frac{\partial \ln\gamma_2^{l}}{\partial T}\right] \quad \text{... (5)}$$

where $\ln\gamma_i^{l}$, x_i and $\frac{\partial \ln\gamma_i^{l}}{\partial T}$ are activity coefficient in liquid state, the mole fraction and variation of log of activity coefficient in liquid state as function of temperature of a component i.

It is evident from equations 3 to 5 that the activity coefficient and its variation with temperature are required to calculate the excess functions. Activity coefficient (γ_i^{l}) could be evaluated by using the equation [15, 16]

$$-\ln\left(x_i \gamma_i^{l}\right) = \frac{\Delta_{fus} H_i}{R}\left(\frac{1}{T_{fus}} - \frac{1}{T_i}\right) \quad \text{…. (6)}$$

 https://doi.org/10.5281/zenodo.14191038

ISSN: 0369-8963

where x_i , $\Delta_{fus}H_i$, T_i and T_{fus} are mole fraction, enthalpy of fusion, melting temperature of component i and eutectic melting temperature, respectively. However, the variation of activity coefficient with temperature could be calculated by differentiating equation 6 with respect to temperature.

$$\frac{\partial \ln \gamma_i^1}{\partial T} = \frac{\Delta_{fus}H_i}{RT^2} - \frac{\partial x_i}{x_i \partial T} \quad \ldots. (7)$$

The value of $\partial x_i / \partial T$ in this expression is used from the phase diagram by taking the slope between two points near the eutectic. The positive values of excess free energy indicate that the interaction between the like molecules (CA−CA and BNB−BNB) are stronger than the interaction between the unlike (CA−BNB) molecule [24].

The solid-liquid interfacial tension plays a key role in a wide range of metallurgical and materials phenomena from wetting [20] and sintering through phase transformations and coarsening [21]. When liquid is cooled below its melting temperature, it does not solidify spontaneously because under equilibrium condition the melt contains the number of clusters of molecules which are of different sizes. As long as the clusters are well below the critical size [22], they cannot grow to form crystals and, therefore, no solid would result. During growth, the radius of critical nucleus is influenced by undercooling as well as the interfacial energy of the surface involved. The interfacial energy (σ) is related to the critical size (r) of nucleus [22] by the following equation:

$$r = \frac{2\sigma T_{fus}}{\Delta_{fus}H.\Delta T} \quad \ldots. (8)$$

 https://doi.org/10.5281/zenodo.14191038

ISSN: 0369-8963

where T_{fus}, $\Delta_{fus}H$ and ΔT are melting temperature, heat of fusion, and degree of undercooling, respectively**.** The interfacial energy (σ) is given by

$$\sigma = \frac{C.\Delta_{fus}H}{(N_A)^{1/3}.(V_m)^{2/3}} \quad \text{…. (9)}$$

where N_A is the Avogadro number, V_m is the molar volume, and parameter C lies between 0.34 and 0.45 [23]. To calculate the molar volume, the density of BCB and CA used was 1.323 and 1.812 g.cm^{-3}, respectively. The calculated values of critical radius and interfacial energy are reported in Table 4 and Table 5, respectively. During the solidification whether droplets nucleate in the melt or on the solid-liquid interface depends on the relative magnitude of three interfacial energies, namely, σ_{SL_1}, σ_{SL_2} and $\sigma_{L_1L_2}$. The interfacial energy σ_{SL_1} and σ_{SL_2} has been calculated using equation (9), however interfacial energy $\sigma_{L_1L_2}$ has been calculated using the equation

$$\sigma_{L_1L_2} = \sigma_{SL_1} + \sigma_{SL_2} - 2\sqrt{(\sigma_{SL_1}\,\sigma_{SL_2})}. \quad \text{…. (10)}$$

where σ_{SL_1}, σ_{SL_2}, and $\sigma_{L_1L_2}$ are the interfacial energies of solid (S) and the liquid L_1, solid (S) and the liquid L_2 , and liquid L_1 and liquid L_2, respectively. It is evident from the Table 5 that the interfacial energies are related by relation

$$\sigma_{SL_2} < \sigma_{SL_1} + \sigma_{L_1L_2} \quad \text{…. (11)}$$

which satisfy the wetting condition and hence it is concluded that the Cahn wetting condition is applicable for the present system.

 https://doi.org/10.5281/zenodo.14191038

ISSN: 0369-8963

3.4. Microstructure

According to Hunt and Jackson [27] the type of growth from melts depends upon the interface roughness (α) defined by

$$\alpha = \xi \Delta_{fus} H/RT \quad \text{... (12)}$$

where ξ is the crystallographic factor whose value lies between 0.5 and 1.0, $\Delta_{fus}H$ is the heat of fusion, T_f is the melting temperature, and R is the gas constant. The value of ξ was used 1.0 for the calculation of α values. The values of α for different materials are reported in Table 2. If $\alpha > 2$ the interface is quite smooth and the crystal develops with a faceted morphology. On the other hand, if $\alpha < 2$, the interface is rough and many sites are continuously available and the crystal develops with a non-faceted morphology. In the present system, the values of α are greater than 2 in all the cases which suggests that the phases grow with facets morphology.

The optical microphotograph of a directionally solidified monotectic has given in Fig. 3a where faceted growth has been observed. The minor component of the monotectic has been shown in the major component as thin lines in the microstructure. The study on interfacial energy reveals the applicability of Cahn non-wetting condition and indicates that both phases are non-wetting to each other.

4. Conclusions

The phase diagram between 4-bromonitrobenzene and 2-cyanoacetamide shows the formation of a monotectic and a eutectic with 0.065 and 0.92 mole fractions of CA, respectively. The diagram shows that the upper consolute temperature is 63.5 ^{o}C above the monotectic horizontal. The growth kinetics suggests that the growth data obey the Hillig-Turnbull equation

 https://doi.org/10.5281/zenodo.14191038

for each material, and the size of critical nucleus depends on the undercoolings. The positive value of enthalpy of mixing suggests the formation of quasi-eutectic structure in the binary melt of the eutectic. Interfacial energies are correlated by the relation $\sigma_{SL_2} > \sigma_{SL_1} + \sigma_{L_1L_2}$, which confirms that the applicability of Cahn's non–wetting condition in the present system. The microstructural investigations show lamellar growth morphology for the eutectic and faceted morphology for the monotectic.

ACKNOWLEDGEMENTS

The authors would like to thank the Rajeev Gandhi Memorial Engineering College and Technology for providing the infrastructure facilities.

 https://doi.org/10.5281/zenodo.14191038

REFERENCES

[1] D. M. Herlach, R. F. Cochrane, I. Egry, H. J. Fecht and A. L. Greer, "Containerless processing in the study of metallic melts and their solidification," *International Materials Reviews,* Vol. 38, No. 6**,** 1993, pp. 273-347

[2] R. Trivedi and W. Kurz, "Dendritic growth," *International Materials Reviews*, Vol. 39, No. 2, 1994, pp. 49-74

[3] B. Majumdar and K. Chattopadhyay, "Aligned monotectic growth in unidirectionally solidified Zn-Bi alloys," *Metallurgical and Materials Transactions A: Physical Metallurgy and Materials Science,* Vol. 31A, No. 7 2000, pp. 1833-1842

[4] M. E. Glicksman, N. B. Singh and M. Chopra, "Gravitational Effects in Dendritic Growth," *Manufacturing in space,* Vol. 11, 1983, pp. 207-218

[5] H. Yasuda, I. Ohnaka, Y. Matsunaga and Y. Shiohara, "In-situ observation of peritectic growth with faceted interface," *Journal of Crystal Growth*, Vol. 158, No. 1/2, 1996, pp. 128-135

[6] P. Gunter, "Nonlinear Optical Effects and Materials, Springer-Verlag," Berlin, 2000, p.540.

[7] N. B. Singh, T. Henningsen, R.H. Hopkins, R. Mazelsky, R.D. Hamacher, E.P. Supertzi, F.K. Hopkins, D.E. Zelmon and O.P. Singh, "Nonlinear optical characteristics of binary organic system," *Journal of Crystal Growth*, Vol. 128, 1993, pp. 976-980.

[8] S. Chaudhary, R.N. Rai, D. Jyothi, U. P. Singh, "Solid state synthesis, thermal, spectral, optical, crystal structure and atomic packing studies of 2-(3-Hydroxyphenyl)-2,3-dihydroquinazolin-4(1H)-one," *Materials Letters*, Vol. 341, 2023, 134253

[9] S. Chaudhary, R.N. Rai, K. Sahoo, M. Kumar, "Forecast of Phase Diagram for the Synthesis of a Complex for the Detection of Cr^{6+} Ions," *ACS Omega,* Vol 7, 2022, 7460–7471

[10] R. N. Rai, S. R. Mudunuri, R. S. B. Reddi, V. S. A. Kumar Satuluri, S. Ganesamoorthy and P. K. Gupta, "Crystal growth and nonlinear optical studies of m-dinitrobenzene doped urea" *Journal of Crystal Growth*, Vol. 321, No.1, 2011, pp. 72-77

[11] M. Prencipe, P. P. Mazzeo, A. Bacchi, "A method to predict binary eutectic mixtures for mechanochemical syntheses and cocrystallizations," *RSC Mechanochem.,* 2025

 https://doi.org/10.5281/zenodo.14191038

[12] J. Rotrekl, J. Abildskov and J. O. Connell, "Molecular correlation function integrals for condensed systems with solid-liquid-liquid equilibria," *Journal of Molecular Liquids*, Vol. 365, 2022, 120184

[13] B. Derby and J. J. Favier, "A criterion for the determination of monotectic structure," *Acta Metallurgica*, Vol. 31, No. 7, 1983, pp. 1123-1130

[14] A. Ecker, D. O. Frazier, and J. I. D. Alexander, "Fluid flow in solidifying monotectic alloys," *Metallurgical Transactions A: Physical Metallurgy and Materials Science*, Vol. 20A, No. 11, 1989, pp. 2517-2527.

[15] J. A. Dean, "Lange's Handbook of Chemistry," McGraw-Hill, New York, 1985.

[16] S. Chaubey, K. S. Dubey and P. R. Rao, "Aluminum-Cadmium Binary Alloy Phase Diagram," *Journal of Alloy phase diagram*, Vol. 6, 1990, pp. 153-157.

[17] R.N. Rai, "Phase diagram, optical, nonlinear optical, and physicochemical studies of the organic monotectic system: Pentachloropyridine-succinonitrile" *Journal of Materials Research*, Vol. 99, No. 5, 2004, pp.1348-1355

[18] U.S. Rai and R.N. Rai, "Physical chemistry of organic eutectics," *Journal of Thermal Analysis and Calorimetry*, Vol. 53 No. 3, 1998, pp. 883-893

[19] W.B. Hillig and D. Turnbull, "Theory of crystal growth in undercooled pure liquids," J*ournal of chemical physics*, Vol. 24, 1956, pp. 914

[20] D. A. Porter and K. E. Easterling, "Phase Transformation in Metals and Aollys," Vokingham (U. K) co. Ltd., 1982

[21] W.C. Winegard, S. Majka, B.M. Thall and B. Chalmers, "eutectic solidification in metals," *Can. J. Chem.*, Vol. 29, 1951, pp. 320- 327

[22] R. N. Rai and U. S. Rai, "Solid-liquid equilibrium and thermochemical properties of organic eutectic in a monotectic system" *Thermochimica Acta*, Vol. 363, No. 1-2, 2000, pp. 23-28

[23] U.S. Rai, R.N. Rai, J. Cryst. Growth 191 (1998) 234–242

[24] N. Singh, Narsingh B. Singh, U. S. Rai and O. P. Singh, "Structure of eutectic melts; binding organic systems," *Thermochimica Acta* , Vol. 95, No. 1, 1985, pp. 291-293

[25] J. W. Christian, "The Theory of Phase Transformation in Metals and Alloys," Pergamon Press, Oxford, 1965, p. 992

 https://doi.org/10.5281/zenodo.14191038

[26] R. Good, “Generalization of theory for estimation of interfacial energies, *Ind. Eng. Chem*,” Vol. 62, 1970, pp. 54-78

[27] J. D. Hunt and K. A. Jackson, “Binary eutectic solidification,” *Transactions of the Metallurgical Society of AIME*, Vol. 236, No. 6, 1966, pp 843-852

 https://doi.org/10.5281/zenodo.14191038

ISSN: 0369-8963

Caption of figures

Fig. 1: Phase diagram of 4-bromonitrobenzene and 2-cyanoacetamide system

Fig. 2: Linear velocity of crystallization at various degree of undercooling for 4-bromonitrobenzene and 2-cyanoacetamide and their monotectic and eutectic

Fig. 3: Directionally solidify optical microphotograph of 4-bromonitrobenzene —2-cyanoacetamide eutectic (a) and monotectic (b)

 https://doi.org/10.5281/zenodo.14191038

ISSN: 0369-8963

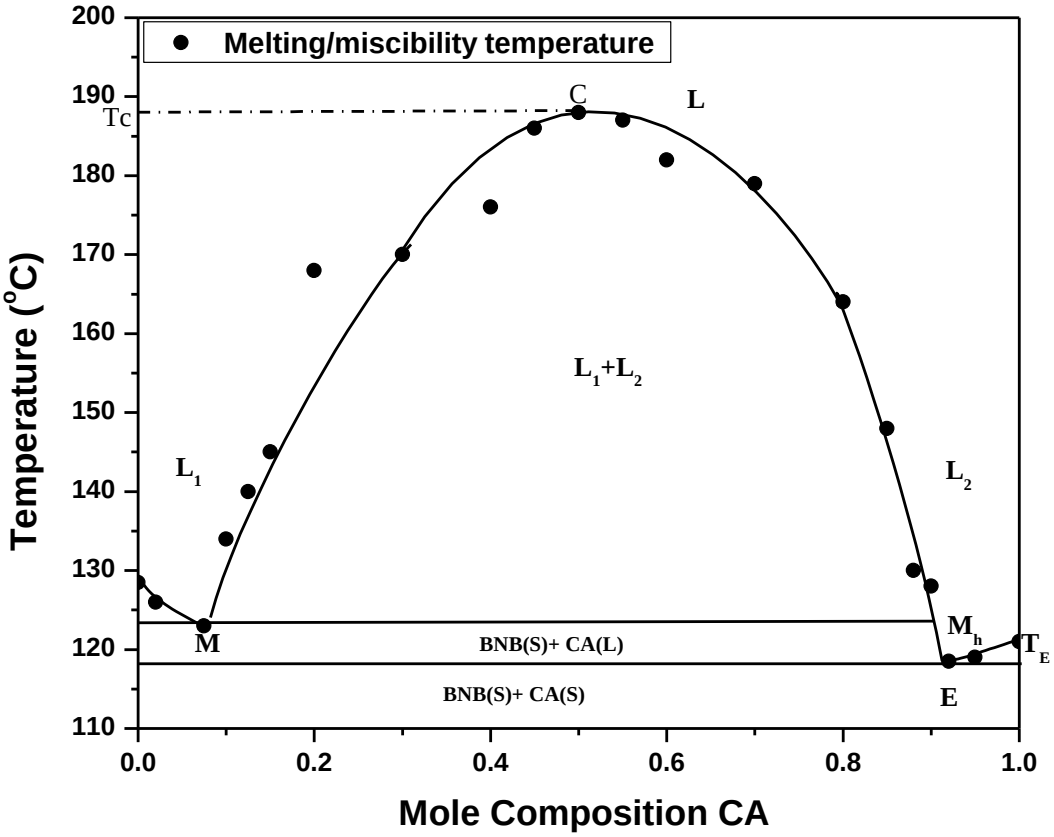

Fig. 1

https://doi.org/10.5281/zenodo.14191038

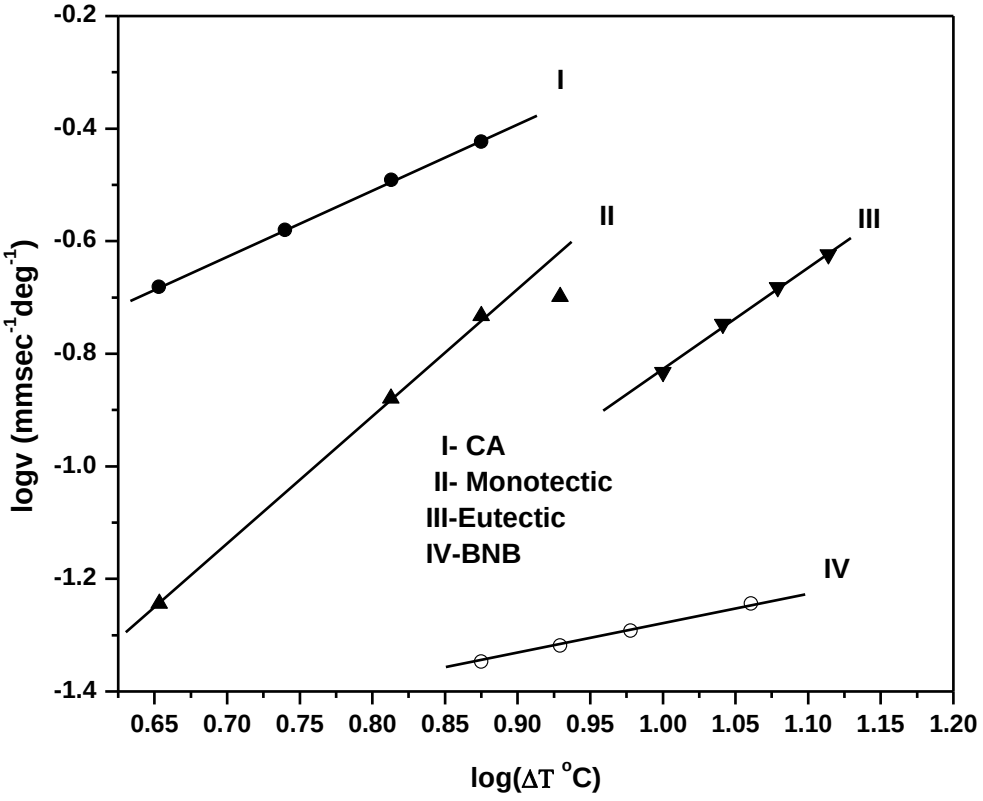

Fig. 2

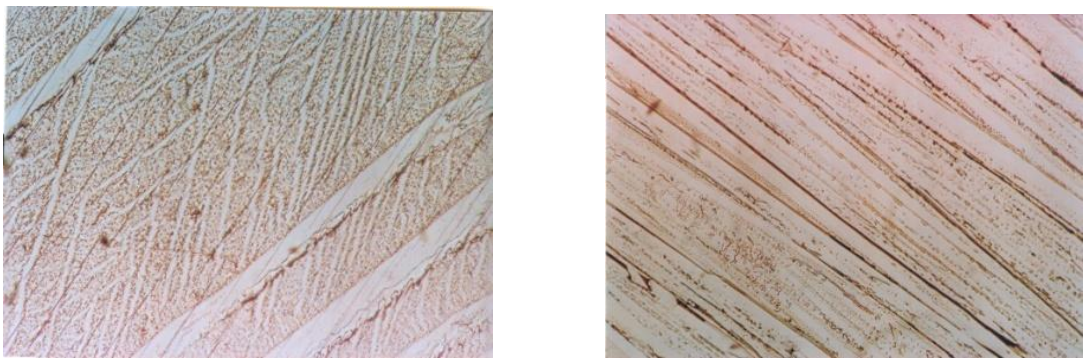

a) b)

Fig. 3

https://doi.org/10.5281/zenodo.14191038

ISSN: 0369-8963

Table 1: Values of ***n*** and ***u*** for pure components, monotectic and eutectic

Material	***n***	***u*(mm sec^{-1}deg^{-1})**
BNB	3.30	63.31
CA	1.17	0.035
Monotectic	-2.58	116.41
Eutectic	1.45	3.51

Table 2: Heat of fusion, entropy of fusion and roughness parameter of BNB, CA and their monotectic and eutectic

Materials	**Heat of fusion (kJ mol^{-1})**	**Heat of mixing (kJ mol^{-1})**	**Entropy of fusion (J mol^{-1} K^{-1})**	**Roughness parameter (α)**
BNB	21.59		48.2	5.8
CA	18.97		40.3	4.9
Monotectic (Exp.)	19.72		42.1	5.1
Eutectic (Exp.)	20.13	0.95	38.9	4.7
(Cal.)	19.18			

Table 3: Excess thermodynamic functions for the eutectic

Material	g^E (kJ mol^{-1})	h^E (k J mol^{-1})	s^E (J mol^{-1} K^{-1})
BNB-CA eutectic	2.80	134.06	0.3353

https://doi.org/10.5281/zenodo.14191038

Table 4: Interfacial energy of 4-bromonitrobenzene and 2-cyanoacetamide and their eutectic and monotectic

Parameter	**Interfacial energy (ergs cm^{-1})**
σ_{SL_2} (CA)	51.48
σ_{SL_1} (BNB)	42.62
$\sigma_{L_1L_2}$ (BNB-CA)	0.42
σ_E (BNB-CA)	50.77

Table 5: Critical radius of 4-bromonitrobenzene and 2-cyanoacetamide their eutectic and monotectic

Undercooling	**Critical radius x 10^{-8} (cm)**			
ΔT (^0C)	CA	BNB	Monotectic	Eutectic
4.5	4.757		0.0376	
5.5	3.892			
6.5	3.293		0.0261	
7.5		2.076	0.0225	
8.5		1.833	0.019923	
9.5		1.640		
10				1.975
10.5		1.484		
11				1.645
11.5		1.484		
12				1.646
13				1.519

 https://doi.org/10.5281/zenodo.14191038